Gravity assisted recovery of liquid xenon at large mass flow rates

L. Virone, S. Acounis, N. Beaupère, J.-L. Beney, J. Bert, S. Bouvier, P. Briend, J. Butterworth, T. Carlier, M. Chérel, et al.

▶ **To cite this version:**

L. Virone, S. Acounis, N. Beaupère, J.-L. Beney, J. Bert, et al.. Gravity assisted recovery of liquid xenon at large mass flow rates. Nuclear Instruments and Methods in Physics Research Section A: Accelerators, Spectrometers, Detectors and Associated Equipment, 2018, 893, pp.10-14. 10.1016/j.nima.2018.02.097 . hal-01758238

HAL Id: hal-01758238
https://hal.science/hal-01758238

Submitted on 30 Jan 2020

HAL is a multi-disciplinary open access archive for the deposit and dissemination of scientific research documents, whether they are published or not. The documents may come from teaching and research institutions in France or abroad, or from public or private research centers.

L'archive ouverte pluridisciplinaire **HAL**, est destinée au dépôt et à la diffusion de documents scientifiques de niveau recherche, publiés ou non, émanant des établissements d'enseignement et de recherche français ou étrangers, des laboratoires publics ou privés.

Gravity assisted recovery of liquid xenon at large mass flow rates

L. Virone [a,*], S. Acounis [a], N. Beaupère [a], J.-L. Beney [a], J. Bert [b], S. Bouvier [a], P. Briend [c], J. Butterworth [c], T. Carlier [d,e], M. Chérel [d,e], P. Crespi [c], J.-P. Cussonneau [a], S. Diglio [a], L. Gallego Manzano [a], D. Giovagnoli [b], P.-B. Gossiaux [a], F. Kraeber-Bodéré [d,e], P. Le Ray [a], F. Lefèvre [a], P. Marty [f,g], J. Masbou [a], E. Morteau [a], G. Picard [a], D. Roy [a], M. Staempflin [c], J.-S. Stutzmann [a], D. Visvikis [b], Y. Xing [a], Y. Zhu [a], D. Thers [a,*]

[a] *SUBATECH, IMT Atlantique, CNRS/IN2P3, Université de Nantes, 44307 Nantes, France*
[b] *INSERM, UMR1101, LaTIM, CHRU Morvan, 2 avenue Foch, Brest, 29600, France*
[c] *AIR LIQUIDE Advanced Technologies Division, 2 rue Clémencière, F-38360 Sassenage, France*
[d] *Centre Hospitalier Universitaire de Nantes, 1 place Alexis-Ricordeau, 44093 Nantes, France*
[e] *CRCINA, INSERM, CNRS, Université d'Angers, Université de Nantes, France*
[f] *CEA, LITEN, DTBH, SCTR, LER, 17 rue des Martyrs, F-38054 Grenoble, France*
[g] *LEGI, Grenoble Alpes University/Grenoble-INP/CNRS, BP53, Grenoble F-38051, France*

We report on a liquid xenon gravity assisted recovery method for nuclear medical imaging applications. The experimental setup consists of an elevated detector enclosed in a cryostat connected to a storage tank called ReStoX. Both elements are part of XEMIS2 (XEnon Medical Imaging System): an innovative medical imaging facility for pre-clinical research that uses pure liquid xenon as detection medium. Tests based on liquid xenon transfer from the detector to ReStoX have been successfully performed showing that an unprecedented mass flow rate close to 1 ton per hour can be reached. This promising achievement as well as future areas of improvement will be discussed in this paper.

1. Introduction

Over the past decades, researchers have employed pure liquid xenon in many different fields including astrophysics, particle physics and medical imaging techniques because of its intrinsic radiation detection properties. In particular, Liquid Xenon Time Projection Chambers (LXeTPC) represents an ideal option for γ-ray detectors in a wide energy range from several tens of keV to tens of MeV [1].

LXeTPC detectors require a sophisticated and reliable cryogenic infrastructure [1]. The cooling system, located remotely from the detector (enclosed in a cryostat), includes a pulse tube refrigerator coupled to a copper cold finger [2] or a specific exchanger supplied by liquid nitrogen [3]. Moreover, as discussed in [4,5], the required level of xenon impurity (O_2 equivalent) must be kept on the order of ppb or even lower. In particular, commercial getters working at "high" temperature (>300 K), plumbing, counter-current coaxial exchanger and double-diaphragm pump are suitable for this purpose [6].

Most Liquid Xenon (LXe) facilities include a storage equipment, that may also work during a detector extended shutdown, to keep the xenon safe. The need of a safe and efficient cryogenic procedure to recover the liquid xenon toward the storage tank strongly impacts the facility design. For small or medium detectors such as XAMS [7] or XEMIS1 [8], a cryopumping operation in bottles is enough for the xenon recovery. However, bigger facilities with hundreds kilograms of liquid xenon such as XENON1T [9], MEG [10], XMASS [11], LUX [6] or XEMIS2 (Section 2.2) require another approach. One solution consists in the development of a "liquid xenon storage system employing the zero boil-off condition" [12]: the liquid xenon vaporization rate (boil-off), generated by all the heat losses, is balanced by the condensation rate of xenon vapors by means of the cooling system. Furthermore, a cryogenic centrifugal pump may also be used for liquid xenon recovery [13].

We have carried out the commissioning of the XEMIS2 facility: it includes the implementation of the liquid xenon recovery process. XEMIS2 is an innovative system designed for 3γ pre-clinical imaging of small animals in hospital centers [8]. It uses nearly 200 kg of pure

* Corresponding authors.
E-mail addresses: virone@subatech.in2p3.fr (L. Virone), thers@subatech.in2p3.fr (D. Thers).

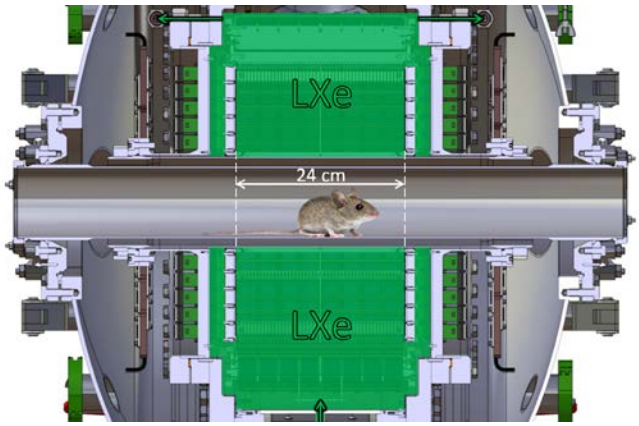

Fig. 2.1. Cut view of the detector: the LXe volume is visible.

liquid xenon. Due to specific design choices, the liquid xenon recovery is gravity assisted. This method safely enables unprecedented transfer rates.

This paper focuses on the liquid xenon transfer from the cryostat to the storage vessel (ReStoX) with special emphasis on the experimental conditions and transfer rate. It is organized as follows: Section 2 presents the XEMIS2 facility, its condenser and the heat losses of ReStoX; Section 3 describes the liquid xenon transfer method using a theoretical approach, experimental results and discussions; finally the conclusion and prospectives are given in Section 4.

2. The XEMIS2 cryogenic facility

2.1. The XEMIS2 detector and infrastructure

Following the success of XEMIS1: a small LXeTPC that showed the potential of the 3γ imaging technique [14], a larger monolithic pure liquid xenon (at 1.2 bar abs and 168 K) cylindrical camera, XEMIS2, for pre-clinical applications is under construction. With a long 24 cm axial field of view, the XEMIS2 detector entirely surrounds the small animal (Fig. 2.1). The detector active volume is covered by $1''$ Hamamatsu PMTs to detect the VUV scintillation photons generated from γ-ray interactions within the xenon. Moreover, the ionization electrons are detected by two circular segmented anodes located at the edges of the detector. The compact XEMIS2 camera also includes a fast DAQ, a traditional purification system and a storage tank called ReStoX assuring the "zero boil-off condition".

The cryogenic infrastructure consists of an elevated low pressure cryostat (< 2 bar abs) surrounding the camera, a high pressure resistant (71 bar abs) storage tank (ReStoX) and a purification loop (Fig. 2.2). Since XEMIS2 is intended to be employed in a hospital center, compactness, convenience of use and safety criteria must be respected. A particular attention is devoted to the vulnerability of the cryostat to pressure rise. To overcome any possible damage to the detector induced by an unexpected pressure increase, we consider a gravity assisted recovery. The liquid xenon transfer toward ReStoX is a simple and reliable operation explained in Section 3.2.

2.2. The XEMIS2 tank storage ReStoX

ReStoX is a cryogenic tank. It controls the overall system pressure. The metallic structure of ReStoX is easily cooled by a massive aluminum condenser located on the top of ReStoX. This exchanger includes two liquid nitrogen coils in which nitrogen film boiling occurs. It offers a temperature adaptation between the nitrogen and the xenon boiling points. The available cooling power is proportional to the nitrogen mass flow rate for a nominal temperature of 170 K. The condenser features a wide cooling power range: from a few W up to 11 kW limited by the exchange surface. Due to their high heat capacity and mass, the condenser (260 kg) and ReStoX structure (440 kg) have an important thermal inertia. Consequently, thermal transient heat loss of ReStoX will not significantly affect the pressure of the facility.

ReStoX pressure is governed by the heat losses and the applied cooling power. Consequently, its pressure can be increased or decreased by adjusting the heat losses balance. A preliminary warm-up test during its storage phase provides an estimation of the heat losses in the condenser, the metallic shell and the xenon. The three later warm-up were slow enough to consider a constant thermal equilibrium over their entire surface. This is justified by the small temperature gradient close to 1 K measured between the top and bottom of ReStoX.

The temperature rise curve was analyzed using the National Institute of Standards and Technology data [15] for the aluminum block, stainless steel vessel and xenon properties. The enthalpy/energy differences are directly calculated from temperatures variations for several time periods of 6 h (Fig. 2.3).

We notice a global heat flux of 17.3 W. Specifically, we estimate a net flux of 7.5 W, 6.8 W and 3.0 W for the aluminum block, stainless steel structure and xenon respectively. As expected, the latter is low: less than 20% of the total: it represents a tiny xenon boil-off rate of 0.03 $g{\cdot}s^{-1}$. Finally, by adding the heat losses of the cryostat (84 W) and the purification circuit (15 W) we determine a net flux, or an equivalent cold power, close to 116 W dispensed by the condenser in normal regime.

3. Liquid xenon transfer: filling & draining of the cryostat

3.1. Cryostat filling procedure

Before filling the detector, we cool it down by introducing the liquid xenon inside (Fig. 3.1). This stage may happen after an extended

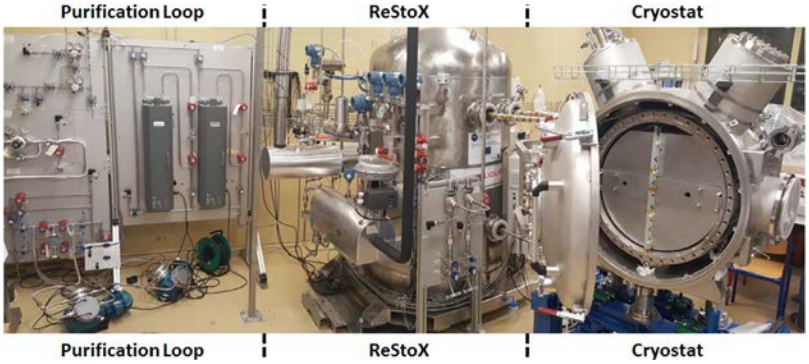

Fig. 2.2. Picture of the XEMIS2 facility with its three subsystems.

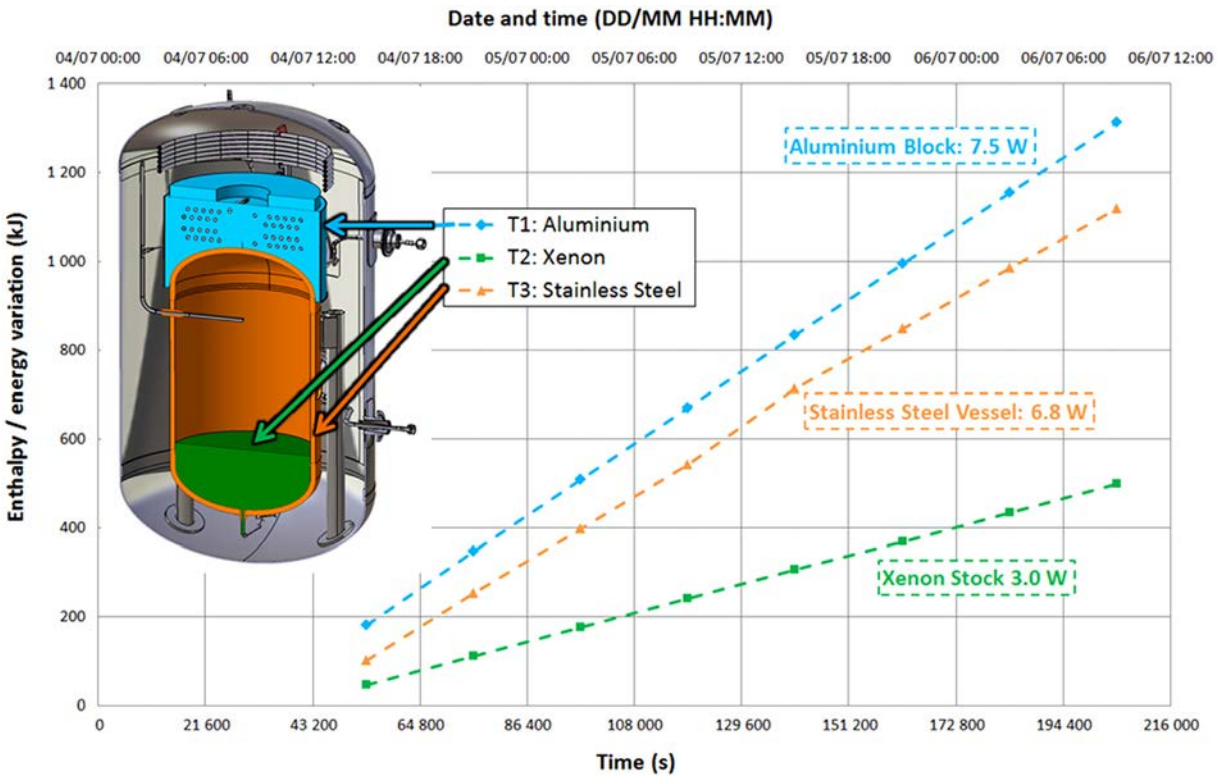

Fig. 2.3. ReStoX warm-up test results to calculate the nominal heat losses in the condenser, the tank/vessel structure and the xenon.

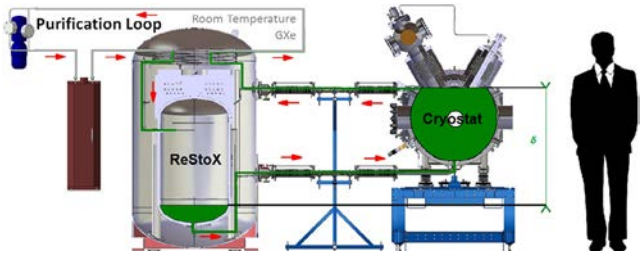

Fig. 3.1. Diagram of the facility in normal regime, once the filling is completed. The xenon flow crosses the three subsystems. The height difference δ, reaching 1.14 m, between the liquid levels is reported.

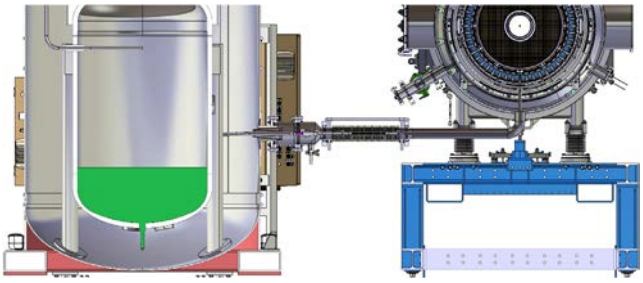

Fig. 3.2. Diagram of the end of the recovery with the empty cryostat.

shutdown with the cryostat at room ambient. For the liquid xenon supply, we rely on the normal ReStoX pressurization to push the fluid through the connection line, equipped with a cryogenic valve, to the cryostat. As a result, the liquid xenon level rises progressively from the inlet orifice to the outlet pipe. The generated xenon boil-off is pumped out of the cryostat by the purification system pump. The boil-off rate should not exceed the capacity of the pump in order to avoid excessive pressure rise in the cryostat. The filling time depends on the enthalpy to be extracted from the cryostat structure, the xenon latent heat of vaporization, and the circulation rate fixed by the purification pump. The xenon pumped flow is set to 3 $g.s^{-1}$, resulting in a mean cooling power of nearly 280 W: a value twelve times superior to the estimated cryostat heat losses in the tested configuration (23 W) (electronics and associated items were not included). Finally we have transferred 44 l of pure liquid xenon, which represents a mass of about 128 kg (Fig. 3.1). The observed cooling/filling duration was approximatively 20 h.

3.2. Liquid xenon gravity assisted recovery

After stabilizing the liquid xenon level within the cryostat, or even during an ongoing filling, we can start the recovery procedure. This operation consists in by-passing the purification loop which disconnects the pumping circuit from the detector and ReStoX. As a result, the gaseous xenon volumes present within ReStoX and XEMIS2 (initial volumic ratio of ∼15) merge. Since the liquid xenon level in the cryostat is higher than the final liquid level within ReStoX, the xenon is transferred from the cryostat to ReStoX by the gravitational force (Fig. 3.2).

If necessary, the operator can easily stop the transfer and re-connects the purification circuit in order to resume the cryostat filling. Both filling and recovery progression are monitored by the ReStoX mass. Once the recovery is completed, we must close the cryogenic valve of the liquid connection line, pump out the remaining gaseous xenon and finally isolate the cryostat from the rest of the facility a few moments later.

To describe the transfer in a simple and intuitive manner, for a turbulent flow, it is possible to use the simplified Eq. (3.1) from [16]. We consider a system composed of different kinds of pipings, fittings and valves. The equation for the transfer is:

$$\frac{P_{cry}}{g.\rho_{LXe}} + \frac{v_{cry}^2}{2g} + z_{cry} = \frac{P_{RSX}}{g.\rho_{LXe}} + \frac{v_{RSX}^2}{2g} + z_{RSX} + L \tag{3.1}$$

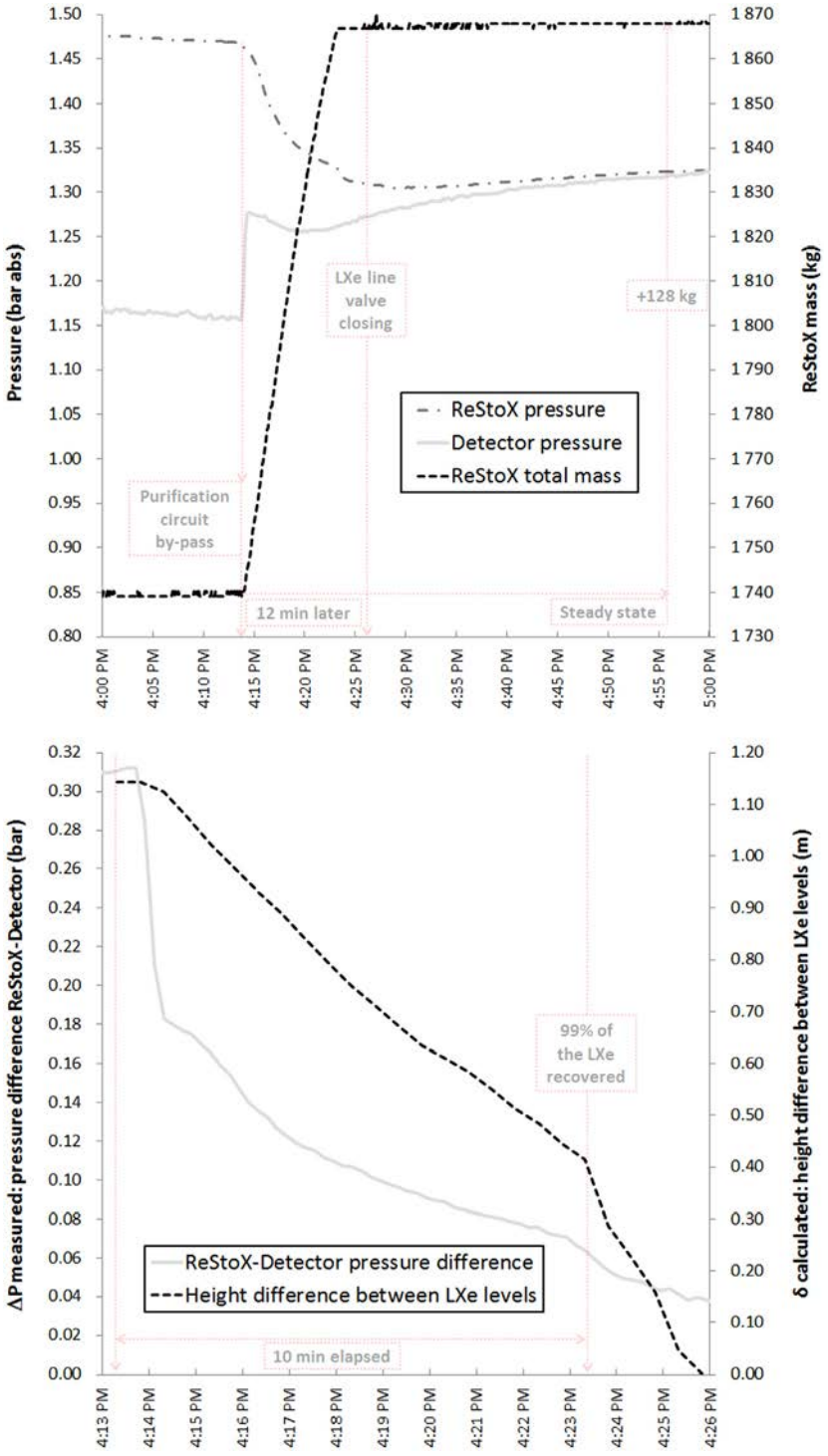

Fig. 3.3. Evolution of ReStoX mass and pressures in each compartment (top): convergence of both pressure and uninterrupted liquid xenon transfer visible. Evolution of pressure difference and height difference between liquid xenon levels throughout the recovery (bottom).

where P_{cry}, P_{RSX}, v_{cry}, v_{RSX}, g and ρ_{LXe} are respectively the instantaneous cryostat pressure, ReStoX pressure, the velocity of the xenon liquid level within the cryostat, within ReStoX, the acceleration of gravity and the liquid xenon average density. Furthermore, we can introduce the parameter that represents the height difference between the LXe/GXe interface inside ReStoX and the cryostat: $\delta = z_{cry} - z_{RSX}$. Lastly, L represents the sum of all straight and punctual load losses (fittings, valves, ...) and may be expressed by Eq. (3.2):

$$L = \sum_i \zeta_i \frac{v^2}{2g} \tag{3.2}$$

where ζ_i depicts pressure drop coefficient of each section of the piping (detailed in [16]). Focusing on δ, Eq. (3.1) leads to:

$$\delta = \frac{P_{RSX} - P_{cry}}{g.\rho_{LXe}} + \frac{v_{RSX}^2 - v_{cry}^2}{2g} + L \Leftrightarrow \delta \simeq \frac{\Delta P}{g.\rho_{LXe}} + L \tag{3.3}$$

assuming that ρ_{LXe} is constant and both v_{cry}^2, v_{RSX}^2 are close and negligible. Thus, the driving force of the transfer is related to the pressure difference ΔP and load losses L which is directly proportional to the square of the instantaneous liquid xenon mass flow rate.

3.3. Experimental results and discussion

We perform the recovery of 128 kg of liquid xenon from the cryostat to the ReStoX tank in 10 min (Fig. 3.3). This corresponds to an equivalent mass flow rate of about 770 kg·h^{-1}.

As expected, we noticed a detector pressure jump when the recovery started. At the same moment, the ReStoX pressure decreased smoothly (merge of the gaseous xenon volumes). The ReStoX total mass rose from 1740 kg (4:14 PM) to 1868 kg (4:24 PM), long before the ReStoX and cryostat pressure equalization (4:55 PM). The pressure difference ΔP decreases more and more slowly even after the valve closing (4:26 PM).

Knowing the geometry of the 2 vessels, the piping and with the measurements of the liquid xenon mass and level within ReStoX, we are able to calculate δ and the liquid xenon outlet velocity or flow rate. Furthermore, each liter of liquid xenon recovered within ReStoX replaces the same volume of vapor. As a consequence, a gaseous xenon circulation is set toward the cryostat. This induced gaseous xenon flow may reach up to 50% of the pumped flow. The pressure difference ΔP includes the load losses related to the xenon vapors displacement.

Minimizing the ΔP or enlarging the pipe diameter (flow losses reduction) could eventually increase the recovery rate.

Moreover, the recovered liquid xenon enthalpy tends to increase whereas the condenser still maintains a constant temperature. This is due to a convective exchange with ReStoX walls (that have a huge heat capacity) at higher temperature. Besides that, the ReStoX pressure is higher than the one of the cryostat.

4. Conclusions

The advantages and potential of using the pure liquid xenon technology is reflected in the increasing number of detectors making use of this innovative technique from particle and astro-particle to medical physics. Independently of the field of use, each system needs an adapted cryogenic infrastructure to liquefy, recover and store the xenon: this offers the opportunity for R&D around the cryogenics. In this context, a crucial point is represented by the capacity of transferring the fluid from the storage tank to the detector vessel and vice-versa without losses and efficiently. In particular, a safe and fast recovery is decisive to avoid any possible problem related to extra heat losses, pressure rise or other cryogenic issues that might happen.

In this context, an assisted pure liquid xenon recovery based on gravity has been implemented and proven to be efficient. Furthermore the liquid xenon, typically three times denser than water, is ideally suited to this kind of transfer. To facilitate this operation, the cryogenic tank that features low heat losses (ReStoX) has a metallic structure that behaves as a big thermal buffer coupled with a condenser capable of operating over a wide range of cooling powers. The elevation of the detector is such that a complete liquid xenon recovery is guaranteed.

The first cryogenic commissioning of XEMIS2 has provided the opportunity to perform recovery tests. It has shown that an unprecedented mass flow rate close to 1 ton·h^{-1} can be reached. In order to further reduce the recovery time, the possibility to better equalize the two pressure vessels and to enlarge the liquid xenon pipe diameter, will be investigated in the future.

Acknowledgments

The research presented in this paper has been funded by the E.U., the Region Pays de la Loire in France and by grants from the French National Agency for Research, "Investisement d'Avenir" ArronaxPlus Equipex no ANR-11-EQPX-0004.

References

[1] E. Aprile, T. Doke, Liquid xenon detectors for particle physics and astrophysics, Rev. Modern Phys. 82 (2010).

[2] E. Hogenbirk, et al., Commissioning of a dual-phase xenon TPC at Nikhef, Nucl. Instrum. Methods Phys. Res. A 840 (2016) 87–96.

[3] S. Slutsky, et al., A xenon condenser with a remote liquid storage vessel, Nucl. Instrum. Methods Phys. Res. A 610 (2019) 669–676.

[4] T. Sumner, et al., The ZEPLIN-III dark matter detector: Instrument design, manufacture and commissioning, Astropart. Phys. 27 (2017) 46–60.

[5] E. Aprile, M. Schumann, et al., The XENON100 dark matter experiment, Astropart. Phys. 35 (2012) 573–590.

[6] F. Wolfs, et al., The Large Underground Xenon (LUX) experiment, Nucl. Instrum. Methods Phys. Res. A 704 (2013) 111–126.

[7] R. Schön, XAMS-Development of Liquid Xenon Detector Technology for Dark Matter Searches (Ph.D. dissertation), Amsterdam University, 2015.

[8] L. Galleg Manzano, Optimization of a Single-Phase Liquid Xenon Compton Camera for 3γ Medical Imaging (Ph.D. dissertation), Ecole des Mines de Nantes, 2016.

[9] E. Aprile, et al., The xenon1t dark matter experiment, 2017. arXiv:1708.07051.

[10] T. Iwamoto, et al., Liquid xenon gamma-ray calorimeter for the MEG experiment, Phys. Procedia 37 (2012) 325–332.

[11] Y. Suzuki, A. Takeda, et al., XMASS detector, Nucl. Instrum. Methods Phys. Res. A 716 (2013) 78–85.

[12] S. Mihara, et al., Development of a large volume zero boil-off liquid xenon storage system for muon rare decay experiment (MEG), Cryogenics 49 (2009) 254–258.

[13] S. Mihara, et al., Development of a method for liquid xenon purification using a cryogenic centrifugal pump, Cryogenics 46 (2006) 688–693.

[14] J.-P. Cussonneau, et al., 3γ medical imaging with a liquid xenon compton camera and ^{44}Sc radionuclide, Acta Phys. Polon. B 48 (2017) 1661–1667.

[15] E. Marquardt, J. Le, R. Radebaugh, Cryogenic material properties database, in: 11th International Cryocooler Conference, Keystone, CO, National Institute of Standards and Technologies, 2000.

[16] R. Bird, W. Stewart, E. Lightfoot, Transport Phenomena, second ed., Hamilton Printing, 2002.